Optically Inaccessible Flow Visualization using Positron Emission Tomography

NMSU PHYSICS DEPT. COLLOQUIUM PRESENTATION

JEREMY BRUGGEMANN

MAY 4TH, 2018

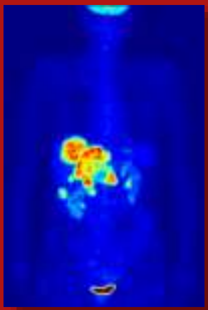
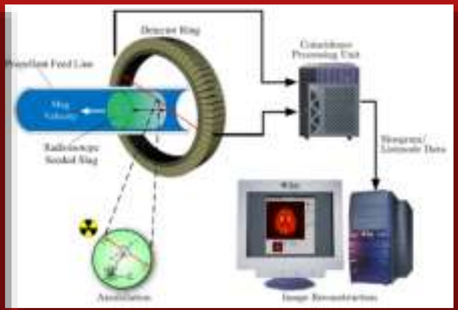
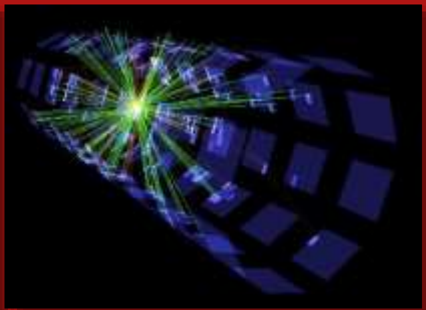

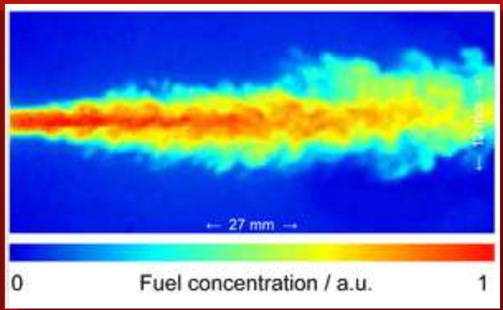

Outline

- Introduction
- Motivation for Positron Emission Tomography
- Background
  - PET Physics & Instrumentation
  - Concept Description
  - Advantages
  - Literature Survey - Optically Inaccessible Flow Visualization
- Experimental Research
  - Objectives
  - Test Methodology
  - Results & Discussion
  - Conclusions
- Current Work – Static Fluid Distribution & Steady State Flow Visualization
- Future Work - Steady State and Periodically Transient Flow Field visualization

Introduction

- Flow visualization is powerful tool in characterizing fluid dynamics in engineering systems
  - Anchor models used for developing system designs
  - Performance characterization using quantitative flow field velocimetry and scalar transport mapping
- Most current techniques require optical accessibility of the flow or probes
  - View ports and probes on integrated systems may not be feasible
    - Compromise structural integrity
    - Intrusive to the flow field
  - Lab scale testing may need to be performed with view ports
    - As built configurations and conditions may deviate from lab scale test conditions
  - Unable to conduct performance anomaly diagnostics, e.g. identify obstructed flow

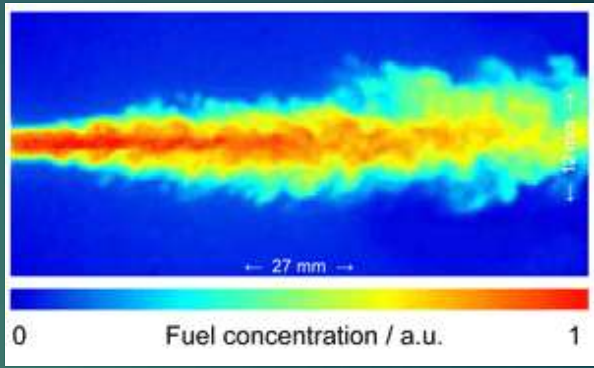

Laser Induced Fluorescence – scalar imaging technique (Source: Ref. 1)

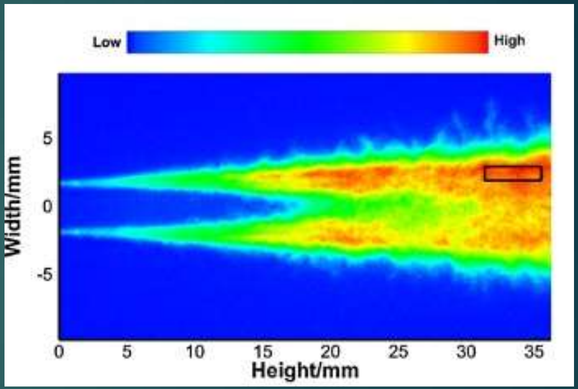

Laboratory-scale optically accessible combustor equipped with a single-element shear coaxial injector (Source: Ref. 2)

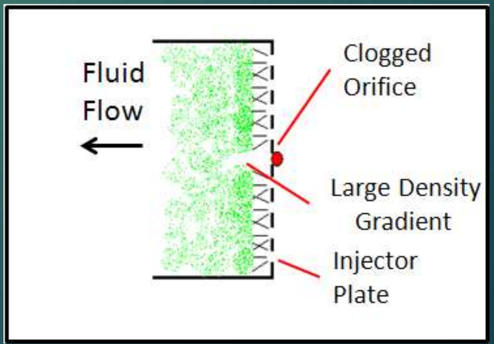

Performance impact due to flow obstruction

Motivation

- Flow visualization of optically inaccessible flows is needed to characterize flow within as-built, integrated systems
- A Possible Solution: Positron Emission Tomography (PET)
  - Used widely in the medical field to non-intrusively visualize 3D fluid distributions in humans and small animals
  - Used to diagnose physiological processes
- PET Technology is becoming more relevant to applications in engineering field
  - Silicon Photo Multipliers (SiPMs)/ Avalanche Photo Diodes (APD) replaces traditional PMTs – increased signal to noise ratio
  - Lutetium Yttrium Oxyorthosilicate (LYSO) scintillation material replacing NaI scintillators
    - Shorter scintillation decay time – reduced dead time
    - Increased gamma-ray stopping power
    - Enables Time-of-Flight (TOF) reconstruction algorithm

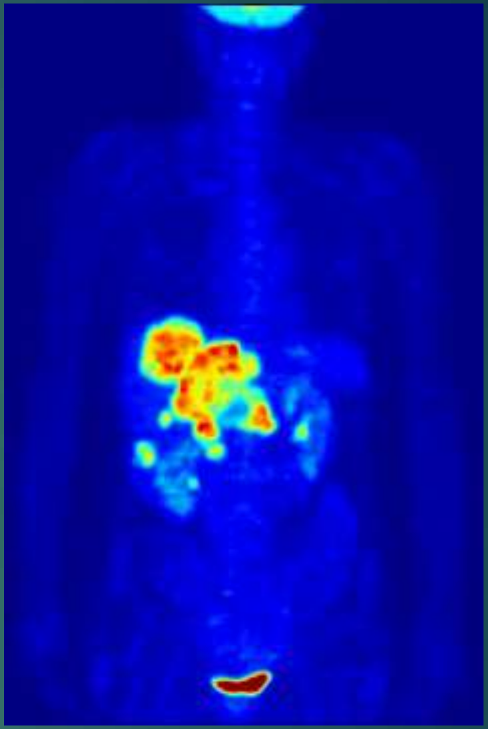

Whole-body PET scan using ^{18}F-FDG (Ref. 8)

2007

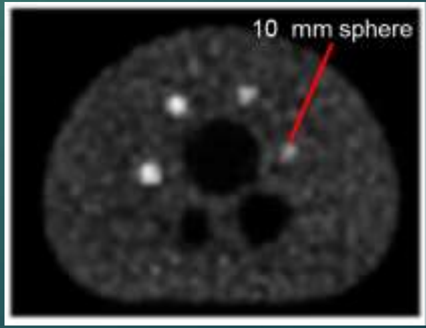

60 Sec Acquisition PET used to image 37 and 28 mm cold spheres, and 22, 17, 13, and 10 mm hot spheres in torso phantom. NOTE: SiPMs not used. (Source: Ref. 3)

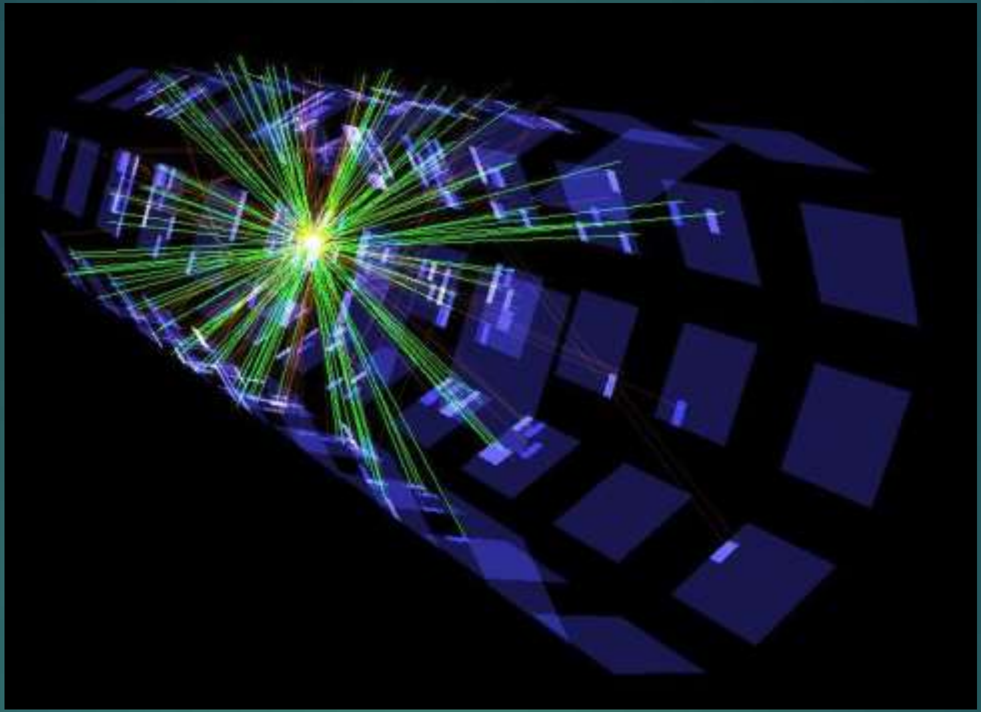

Background

PET PHYSICS & INSTRUMENTATION
CONCEPT DESCRIPTION
ADVANTAGES
LITERATURE SURVEY

PET Physics & Instrumentation

- Beta+ Decay
  - Unstable radioisotopes emit positrons with initial kinetic energy
  - Kinetic energy reduced through interaction with surrounding media until sufficiently low to annihilate with electrons
  - Produces two nearly collinear 511 keV gamma-rays propagating in opposite directions
- PET Detectors
  - Gamma-rays interact (primarily Compton scatter) with scintillating crystals emitting optical photons
  - Optical photons are detected by PMTs/SiPMs
- Single detections are processed to identify coincident detections within specified time window
- Coincident detections = Line of Response (LOR) between triggered detectors
- Multiple LORs and time-of-flight (TOF) data used to reconstruct radioisotope distribution

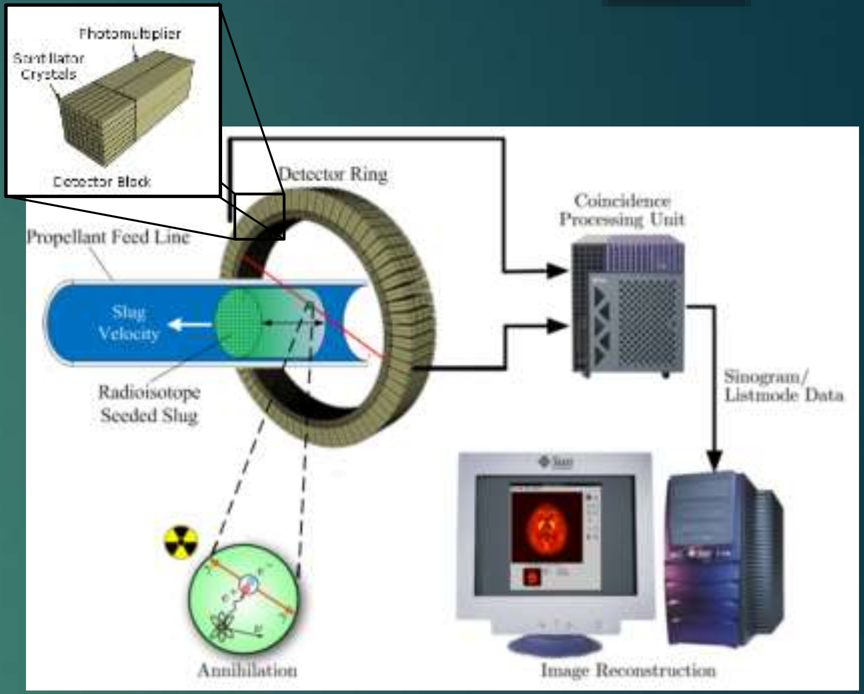

Conceptual schematic of PET applied to visualizing flow in a pipe (Modified from Ref. 8)

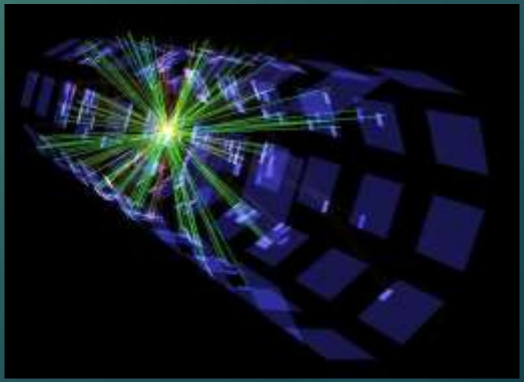

Measured LORs for 3 ml slug of F-18/water solution in Modular Unit at Positron Imaging Centre of Univ. of Birmingham, UK

Concept Description

- General flow visualization concept description
  - Inject Beta+ emitting radioisotopes “In-solution” into flow of interest
    - Utilize radioisotopes of bulk media or compatible constituent
    - Oxygen-15 for oxidizer systems – 2 min. half-life
    - Carbon-11 for hydrocarbon based fuel systems – 20.3 min. half-life
    - Krypton-79 for Krypton based electric propulsion systems – 35 hr. half-life
    - Etc. – many to choose from
  - Utilize PET system to detect back-to-back gamma ray (511 keV) emissions resulting from the decay process
  - Utilize image reconstruction algorithms to generate images of the 3D radioisotope distribution as it traverses the flow of interest
  - Attenuation mapping applied to reconstruction algorithm provided by 3D CAD models for increased resolution

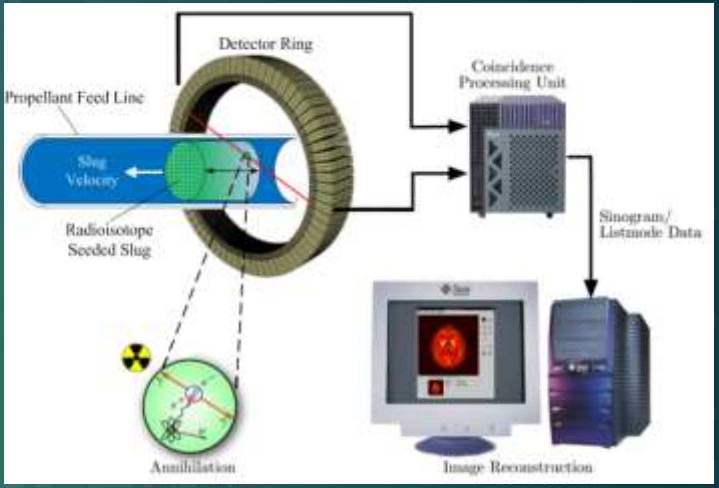

Conceptual schematic of PET applied to visualizing flow in a pipe (Modified from Ref. 8)

Advantages

- Benefits of flow/fluid distribution visualization of optically inaccessible flow fields with PET Technology
  - Gamma rays are highly energetic (511 keV) enabling penetration of fluid containment materials
  - Fluid dynamics of fully integrated systems can be characterized
  - Using radioisotope of the bulk media preserves thermochemical properties during visualization process
  - radiobiological hazards mitigated due to relatively short radioisotope half lives, e.g. 2 minutes for O-15
  - 3D CAD models of engineering system can be superimposed on 3D radioisotope distribution data for high fidelity visualization

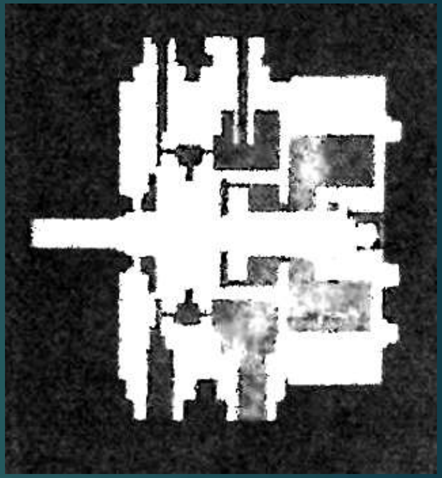

1988 - Bearing rig oil injection visualization – 3D CAD model superimposed (Source: Ref.4)

Literature Survey

- PET application in the Engineering Field
  - 1988 – Visualization of faulty oil injection in bearing rig using Multi-wire Proportional Counter.4
  - 2008 – Visualization of pharmaceutical mixing in steel drums[5]
- Early 1990's to present - Positron Emission Particle Tracking (PEPT) used to characterize particle 3D dynamics in mechanical systems – pioneered at the Positron Imaging Centre (PIC)
  - Variation of traditional PET as only, up to, a few particles are tracked at one time
  - Sub-millimeter sized particles tracked to within 1.5 to 2.0 mm for velocities up to 100 m/s.[7]
    - Lower velocities enable increased precision
  - Draw back: characterizing flows requires a significant number of particles.

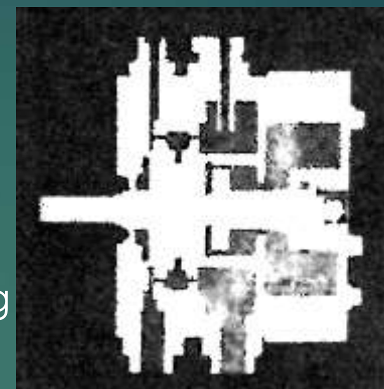

Bearing rig oil injection visualization (left) - 60 minute acquisition (Source: Ref.4)

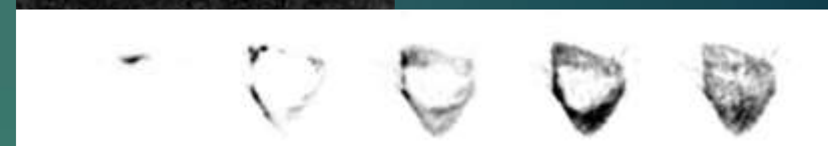

Visualization of pharmaceuticals progressively mixing in 0.3 m diameter steel drums (above) – 20 minute acquisition. (Source: Ref. 5)

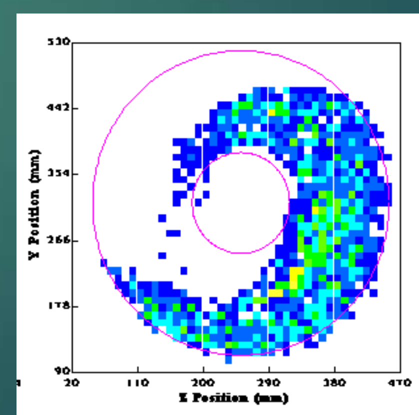

Particle residence times of particle tracked in mechanical mixing system. (Source: Ref. 6)

Literature Survey (cont.)

- Alternate Optically Inaccessible Flow Visualization Techniques
  - Neutron Radiography:
    - 1988 application of Neutron Radiography led to 2D mapping of oil distribution in Rolls Royce Gem Engine
    - Aeration found in return line causing engine oil overfilling and leaking
    - Limited to 2D with occlusion caused by oil build up on engine walls in the foreground
  - Ultrafast Electron Beam X-ray Computed Tomography:
    - 2012 application using X-rays to visualize multiphase flow through pipelines with liquid velocities of up to 1.4 m/s
    - Tests were performed with gas inlet pressures of 2.5 bar
    - Limited to low pressure applications due to order of magnitude larger attenuation coefficient

Rolls Royce Gem Engine oil injection visualization – snap shot of real time acquisition. (Source: Ref.4)

Virtual three dimensional plots of two phase flow obtained using X-ray CT. (Source: Reference 12)

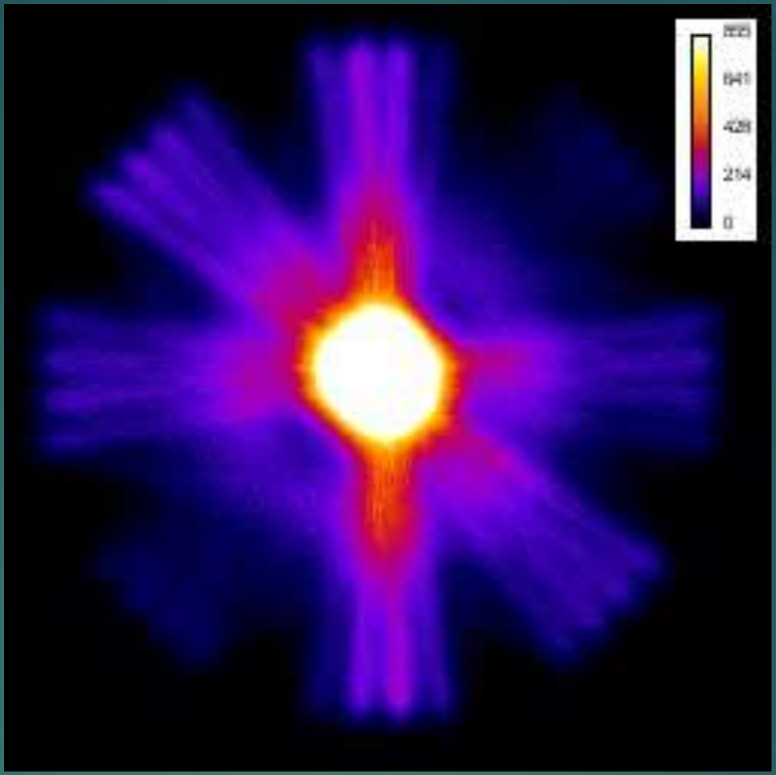

Experimental Research

POSITRON IMAGING CENTRE – UNIVERSITY OF BIRMINGHAM, UNITED KINGDOM

Objectives

- Overall objective: Parametrically bound the applicable flow fields that can be sufficiently visualized using current PET systems
  - Requires characterization of PET systems' dynamic resolution (i.e. achievable spatial resolution using data acquired within a specified unit of time) and count rate performance
- Experiment Objective
  - Measure the dynamic resolution for the ADAC Forte Gamma Camera and Modular PET Unit located at the Positron Imaging Centre
  - Measure the peak count rates for the ADAC Forte Gamma Camera and Modular PET Unit
  - Use measurements to begin establishing a correlation that can be extrapolated to approximate a PET system's dynamic resolution given it's measured Peak NECR

Dynamic Resolution Measurements

General Test Approach

- A fixed volume of Fluorine-18 (F-18)/water solution concealed in a pipe placed in the systems' field of view (FOV)
  - Represents a slug of radioisotope labeled media flowing through a system with laminar flow
- Inactive particles of various sizes placed in the volume
  - Represents a flow feature of interest
- Smallest resolvable particle within a specified acquisition time is the dynamic resolution for that acquisition time
- Test approach 1: ADAC Unit – Volume translated at various velocities through the FOV of the PET scanner
- Test approach 2: Modular Unit – Test volume containing particles remains stationary; Acquisition times used for radioisotope distribution reconstruction varied
  - Quasi-dynamic - assumes that particle does not translate more than half of the particle diameter in the acquisition time.

ADAC Forte Gamma Camera

Modular PET Unit with test apparatus

Test Apparatus

- Fluid containment
  - 10 mL syringe with plunger located at the 3 mL indicator
  - Non-Activated Particles
    - Diameters: 3.0 ± 0.1 mm, 5.0 ± 0.1 mm, 8.0 ± 0.1 mm
    - Adhered to tip of interchangeable syringe plungers
- Syringe with test volume friction fit in steel pipe up to stopping flange
- ADAC - Pipe connected to rotational drum at 140 mm radius (series 1) and 70 mm (series 2 - shown in figure)
- Modular – syringe at single location

3, 5, and 8 mm particles adhered to interchangeable plungers

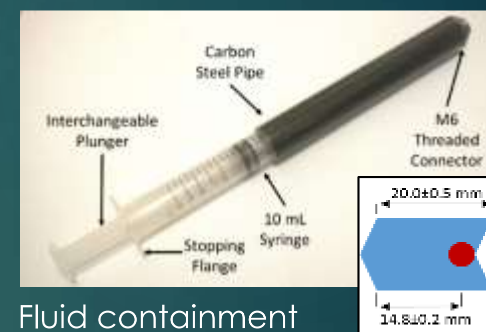

Fluid containment with cross sectional geometry of test volume (inset)

ADAC Unit Test Setup

Modular Unit Test Apparatus

Peak Count Rate Measurement

- Modular Unit - Modified NEMA NU2 Standard Approach for determining Noise Equivalent Count Rate (NECR) Ref. 10
  - Scattering Media: ASTM A511 Steel Pipe with 69.0 ± 0.25 mm O.D., 9.5 ± 0.25 mm wall thickness and 978 ± 1 mm length
- ADACS Gamma Camera – only prompt coincidence count rate measured
  - Scattering media: 20 cm dia. X 20 cm long Nylon cylinder
  - No multiple and random detection measurements available for NECR
- Line Source: filled 2.9±0.1 mm inner diameter polyethylene hose with an F-18/water solution
- Acquisitions taken over several half-lives with line source inside the scattering media

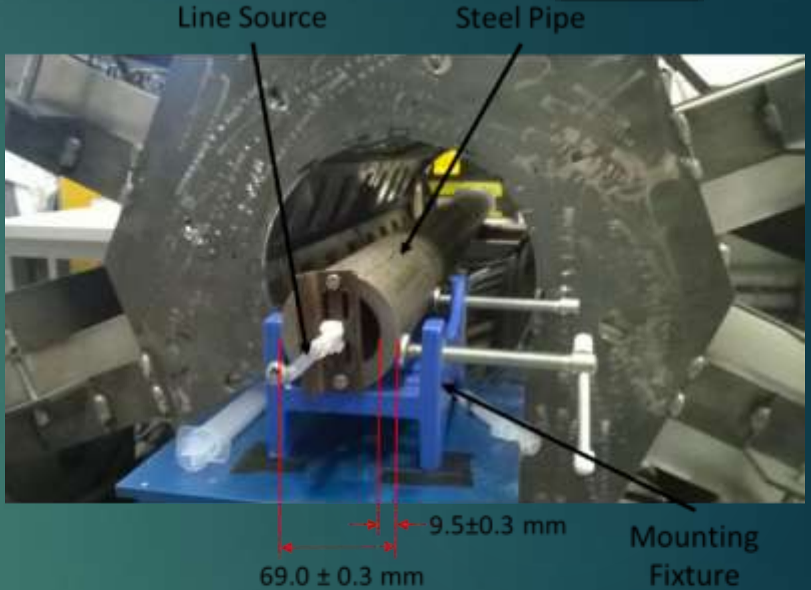

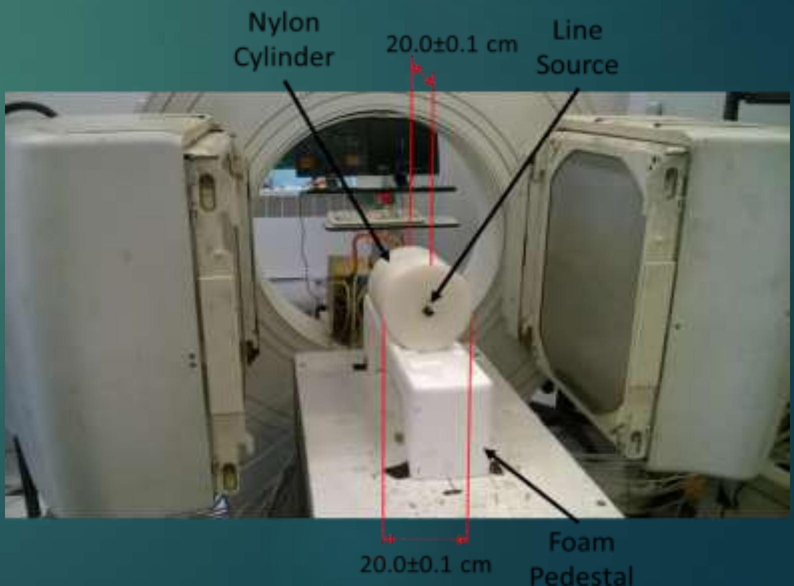

Post-Test Processing

- Image Reconstruction Algorithms
  - ADAC: Simple 2D back projection
    - User specified mid-volume plane, slice thickness and acquisition duration
    - Each projection is 1 mm thick and contains 1 mm x 1 mm pixels
    - Pixel value represents number of LORs that intersected the pixel on the projection plane
  - Modular Unit: simple, 3D back projection
    - Adapted from PEPT algorithm
    - Each voxel intersected by a detected LOR incrementally increased
    - Voxel size: 1 mm x 1 mm x 1mm
  - Disclaimer: Neither algorithm is representative of state-of-the-art nor are they representative of higher performing Filtered Back Projection (FBP) algorithms (standard algorithm used in tomography)

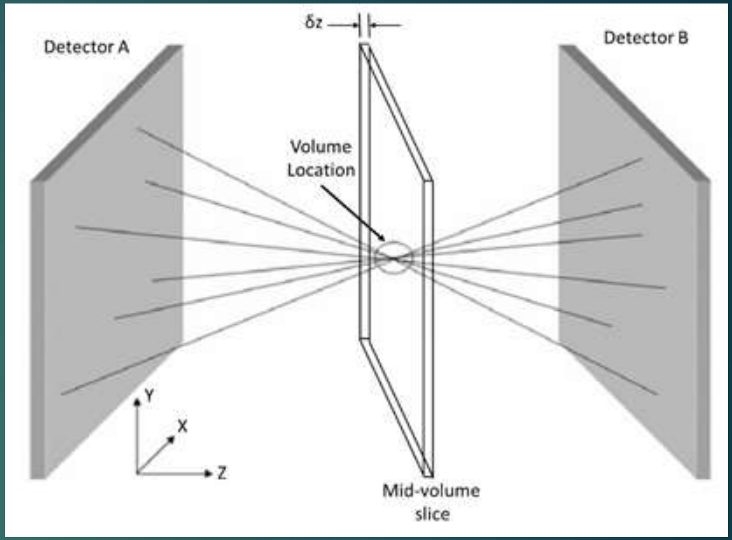

Conceptual schematic of ADAC Unit image reconstruction algorithm (modified from Ref. 5)

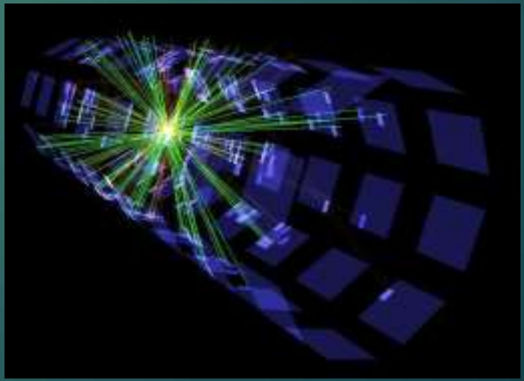

Measured LORs for 3 ml slug of F-18/water solution in Modular Unit

Post-Test Processing

- Intensity spread functions, i.e. profiles, were generated by plotting pixel values along the particles' centerline.
- Reference profile generated using acquisition of activated volume without a particle

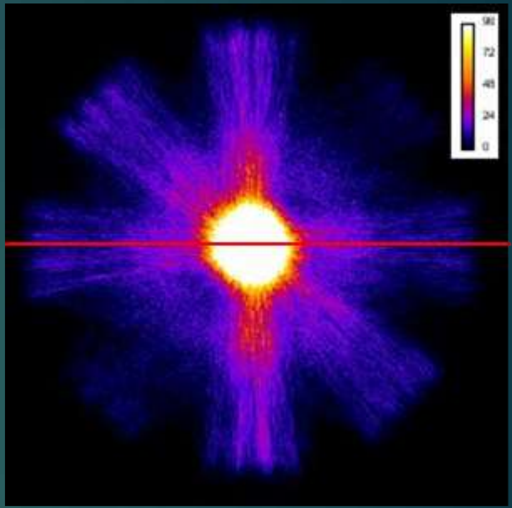

Modular Unit: Particle mid-plane transverse projection

Example of x-axis profile for test volume containing 5 mm particle with 1 second acquisition time plotted against the reference profile

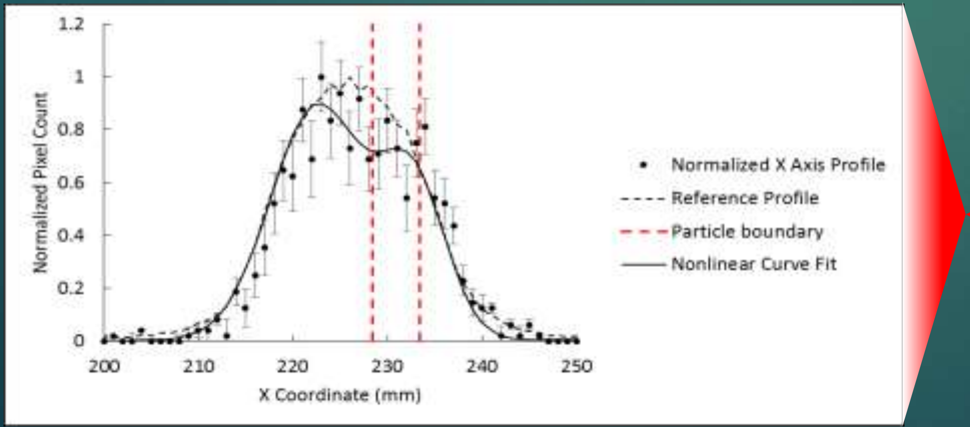

ADAC: Particle mid-plane axial projection

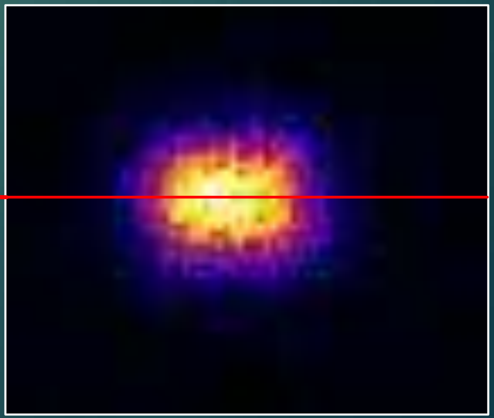

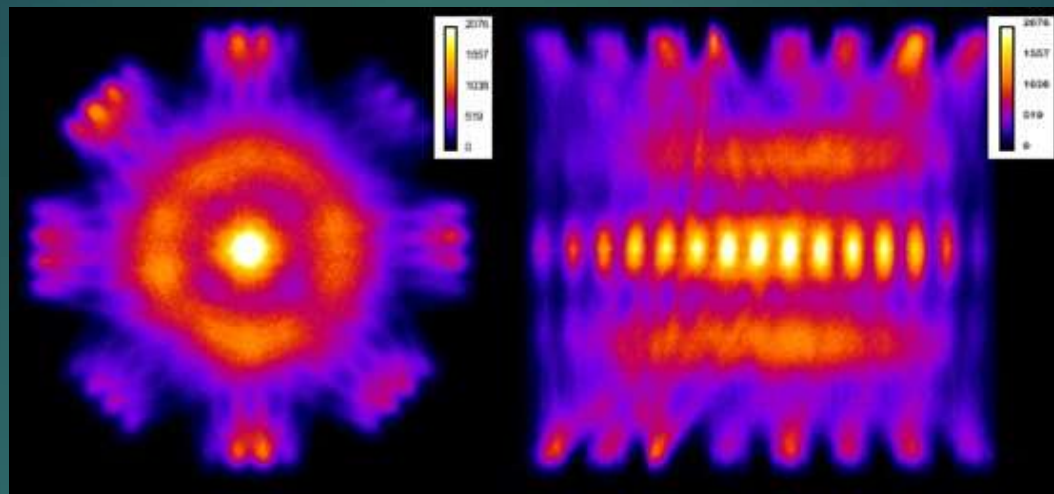

RESULTS AND DISCUSSION

DISCLAIMER: POST PROCESSING RESULTS ARE PRELIMINARY IN NATURE.

Dynamic Resolution Measurements

- ADAC Unit Measurements
  - Volume activity level: 732 μCi (27.1 MBq)
  - Velocity: 0.25 cm/s
  - Particle size: 5 mm
  - Projection plane at BDC at beginning of first full rotation
  - Frame interval: 1 sec (Volume travel during frame interval: ~5 mm)
- Qualitative features indicate particle's presence
  - Evidence of striation (alternating hi-low) caused by reconstruction algorithm – prevents quantitative analysis

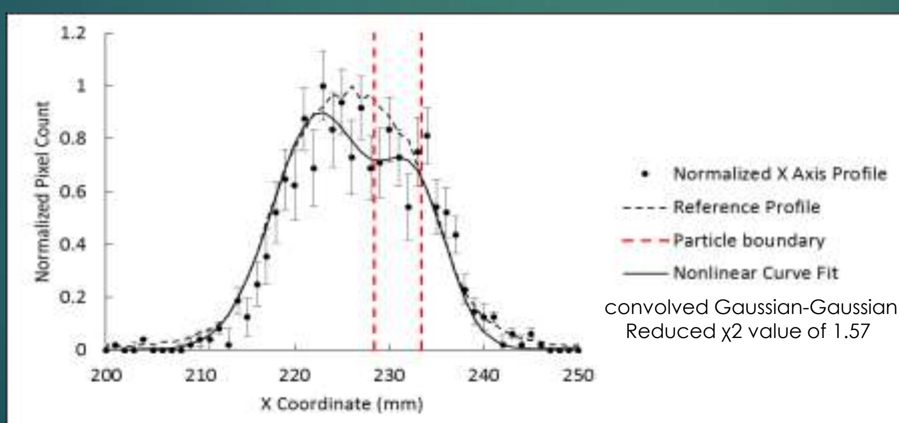

Total count profile along central x axis with curve fit normalized to max reference value

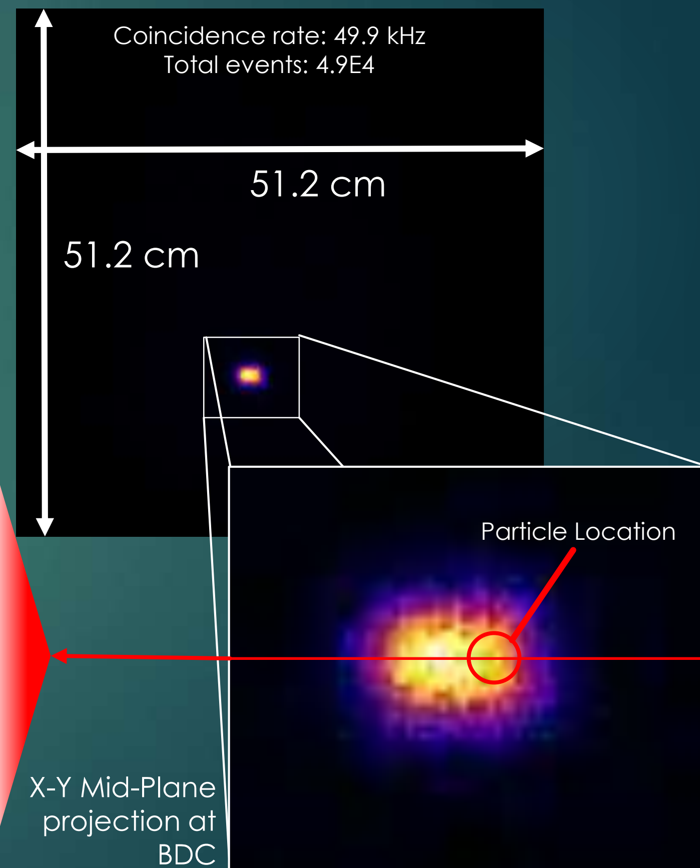

X-Y Mid-Plane projection at BDC

Dynamic Resolution Measurements

- Evaluation of Modular Unit Measurements
  - Mean prompt count rate: 815 kcps
  - Image reconstruction detections: 815000
  - 8 mm particle
  - Projection plane at 8 mm particle mid-particle plane
  - Acquisition interval: 1 sec
  - Particle not resolvable according to FWHM criteria – insufficient statistical correlation

X-Y 8 mm particle Mid-Plane Projection

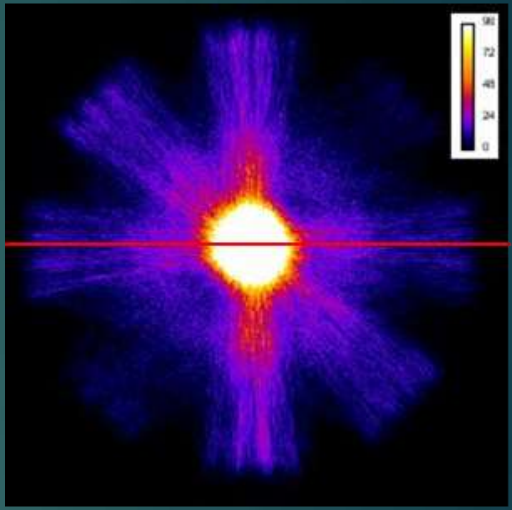

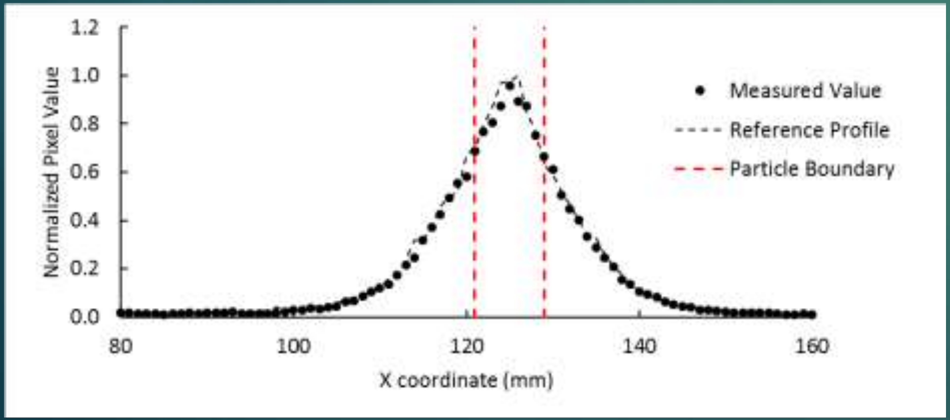

8 mm particle centerline profile in x direction: 1 s acquisition.

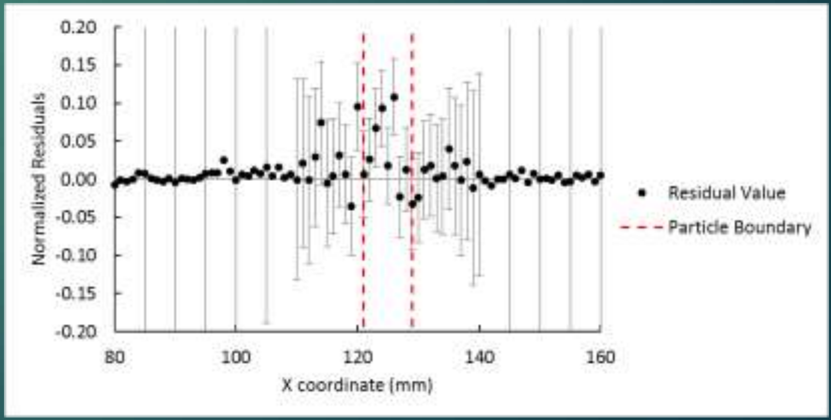

Corresponding residuals

Dynamic Resolution Measurements

- Increased acquisition window for increased detections
  - Mean prompt count rate: 815 kcps
  - Image reconstruction detections: 8,150,000
  - 8 mm particle
  - Projection plane at 8 mm particle mid-particle plane
  - Acquisition interval: 10 sec
  - Effective velocity: 0.04 cm/s
    - Velocity = particle radius / acquisition time
  - FWHM: 6.84 ± 0.31 mm
    - Lower than particle diameter - Suggests inaccurate quantitative results - particle qualitatively resolved

X-Y 8 mm particle Mid-Plane projection

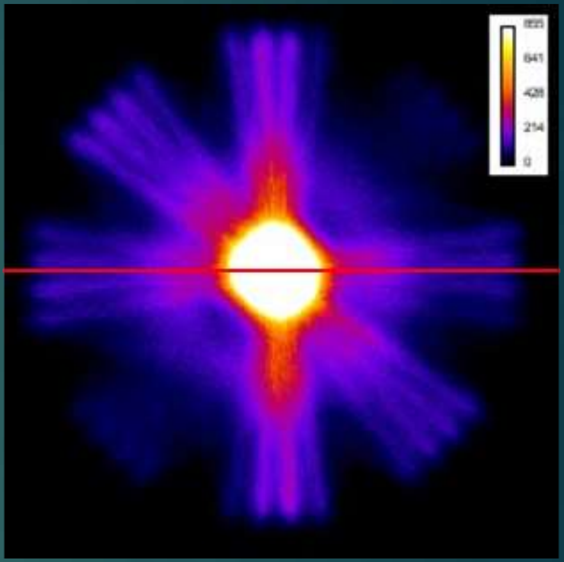

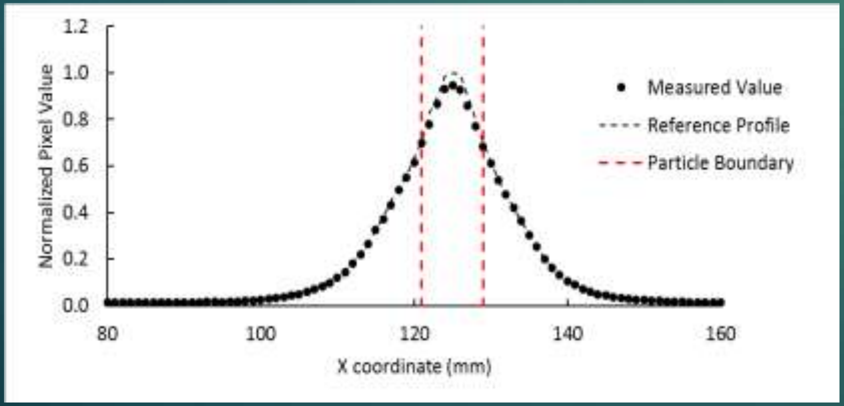

8 mm particle centerline profile in x direction: 10 s acquisition

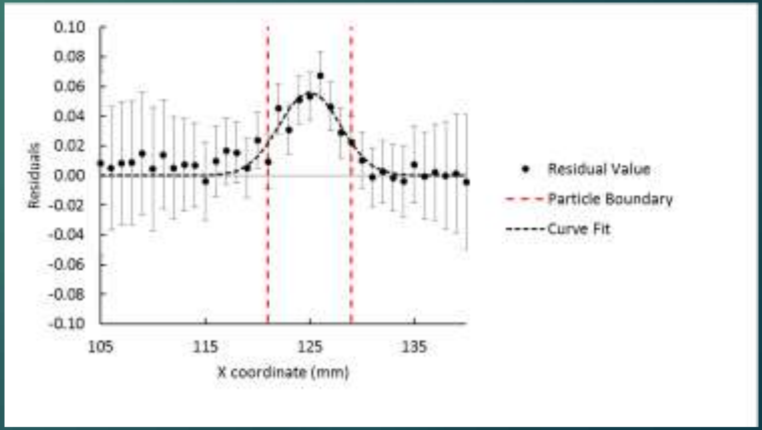

Corresponding residuals

NECR Measurements – Modular Unit

- Peak NECR: 93250 cps
  - Activity: 132.1 µCi/ml (4.89 MBq/ml)
  - Peak NECR Comparable to commercially available PET systems operating in 3D mode (e.g. DSTE and DRX)
  - Specific activity at peak NECR is an order of magnitude larger than DSTE and DRX systems
    - Suspected to be attributed to lower sensitivity due to detector geometry

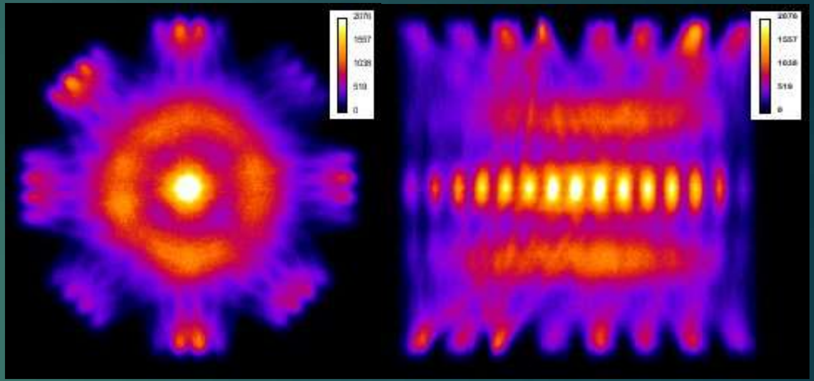

Transvers (left) and axial (right) projection of line source

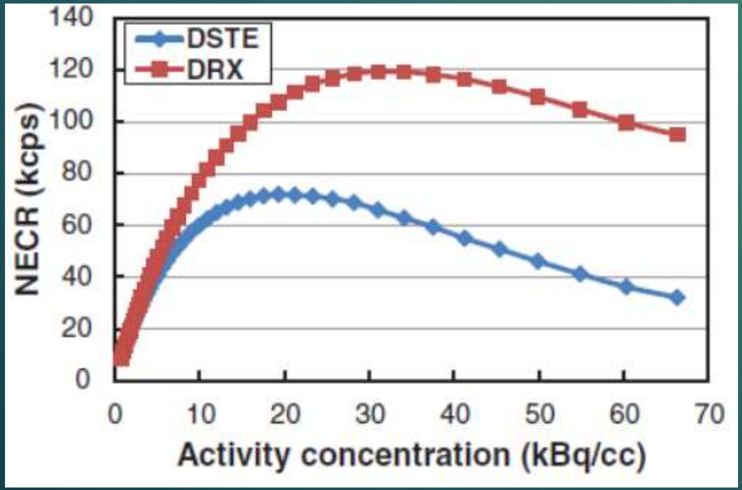

Reference NECR curves for Commercially available systems (Source: Ref. 11)

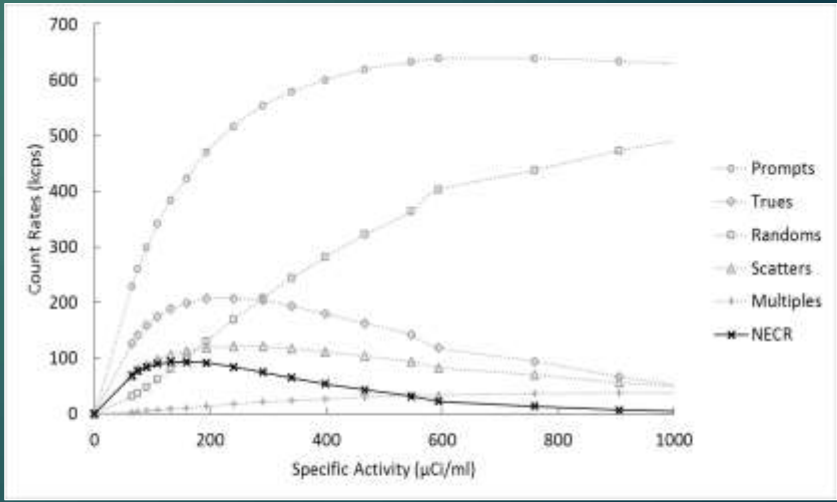

Modular Unit approximate NECR curve

Peak Count Rate Measurement – ADAC Unit

- Only Prompt Coincident Count Rate measured
  - Randoms and multiples measurements not available
- Peak Prompt Count Rate: ~63,000 cps
- Peak NECR must be below this count rate.

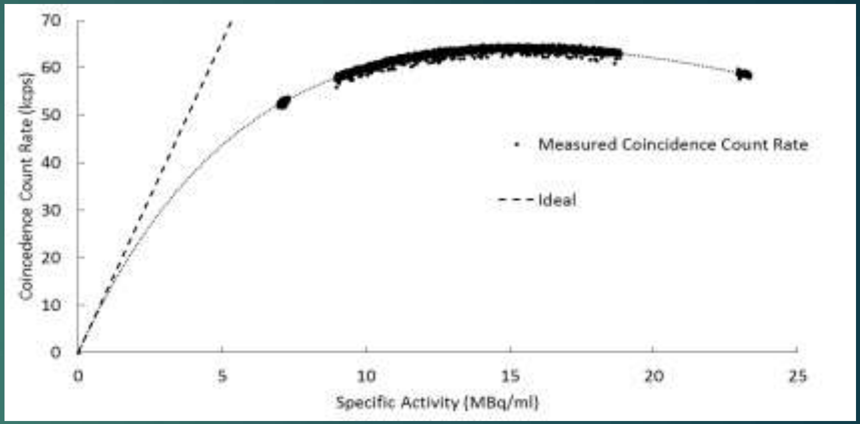

ADAC Unit optimal specific activity curve

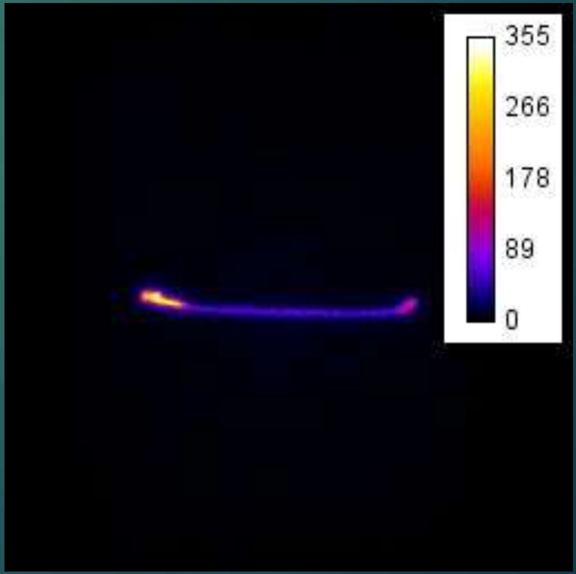

Axial projection of line source used for ADAC count rate measurement

Dynamic Resolution – Peak Count Rate Correlation

- Research to this point has only produced two rudimentary data points – Shown in table.
- Lower dynamic resolution of modular unit despite higher peak count rate
  - Attributed to lower performing modular unit reconstruction algorithm
- Key note: Peak NECR alone is not sufficient metric for cross PET system comparison
  - Reconstruction algorithm needs to be considered and standardized across all system comparisons
  - Investigating use of sinogram-based FBP reconstruction algorithm
    - Difficult to implement for the ADAC since it is a "gamma camera" with non-axisymmetric detector configuration

Table. Tabulated results of dynamic resolution and peak count rate measurements.

System		**ADAC***	**Modular**
Peak Count Rate (kcps)		63	93.3
Resolvable Particle (mm)		5	8
Acquisition Time (sec)		1	10
Velocity (cm/s)		0.25	0.04
Specific Activity	(kBq/mL)	15000	4890
	μCi/mL	405.4	132.2

* ADAC unit peak count rate is based on prompt coincident count rates and is only intended to reflect a maximum possible count rate.

Conclusions

- Testing was performed to measure the dynamic resolution and peak count rate of the ADAC Forte Positron Camera and the Modular Unit located at the Positron Imaging Centre.
  - Limitations from both reconstruction algorithms prevented quantitative resolution of the particles
  - Qualitative indications in the particle center line profiles were used to facilitate cross system comparison between ADAC and modular units
  - Preliminary results indicate that, despite the modular units superior count rate performance, the higher performing ADAC image reconstruction algorithm enabled the ADAC unit to have a higher dynamic resolution.
- No dynamic resolution – peak count rate correlation established for cross system comparison
  - Standardized image reconstruction algorithm needs to be implemented

Current Work

STEADY STATE FLUID FLOW & STATIONARY FLUID DISTRIBUTION VISUALIZATION

Steady-State Incompressible Fluid Flow

- Dynamic Resolution – Peak Count Rate Correlation work continued through simulation. –
  - Modified to orifice flow to facilitate follow on testing
- Simulate radioisotope labeled flow through an orifice using computational fluid dynamics (CFD)
  - Species transport simulated with hyperbolic differential equation solver
  - Orifice sizes varied – analogous to varied particle sizes in UofB testing.
  - Radioisotope concentrations will be varied
  - Initial series will simulate flow of water/F-18 solution
  - Radioisotope concentration distribution output passed to GEANT4 Monte-Carlo based physics package for detector response simulation.

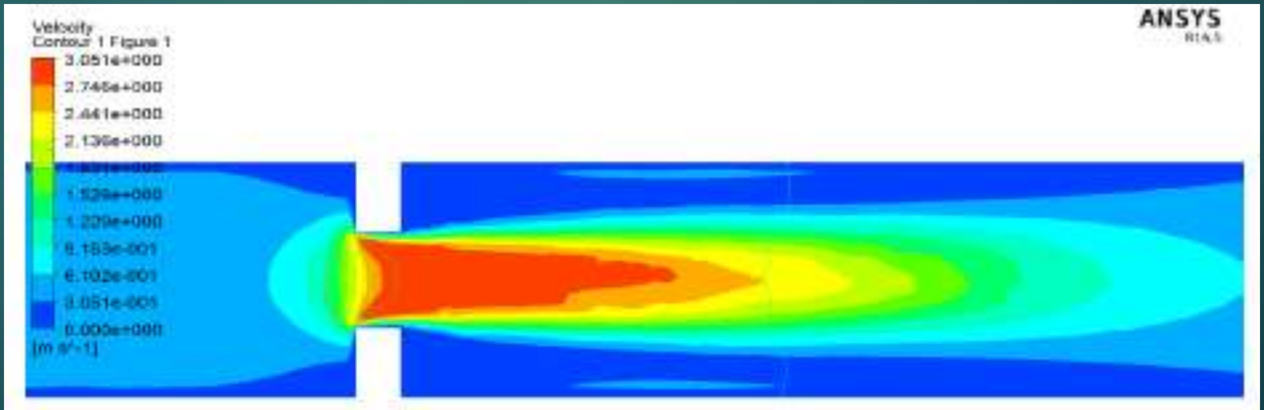

CFD Simulation results for incompressible fluid flow through an orifice. (Source: Ref. 13)

Steady-State Incompressible Fluid Flow

- Monte Carlo based simulation of detector response for each time-slice of the CFD output
- Simulation tool: GATE (GEANT4 Applications for Tomographic Emissions)
  - Versatile, comprehensive PET system simulation software.
- GEANT4 primary kernel
  - Applications layer allows users to define PET System specific simulations
- Capable of modeling time dependent phenomena allowing the simulation of time curves under realistic acquisitions
  - Detector/source movements
  - Source decay kinetics

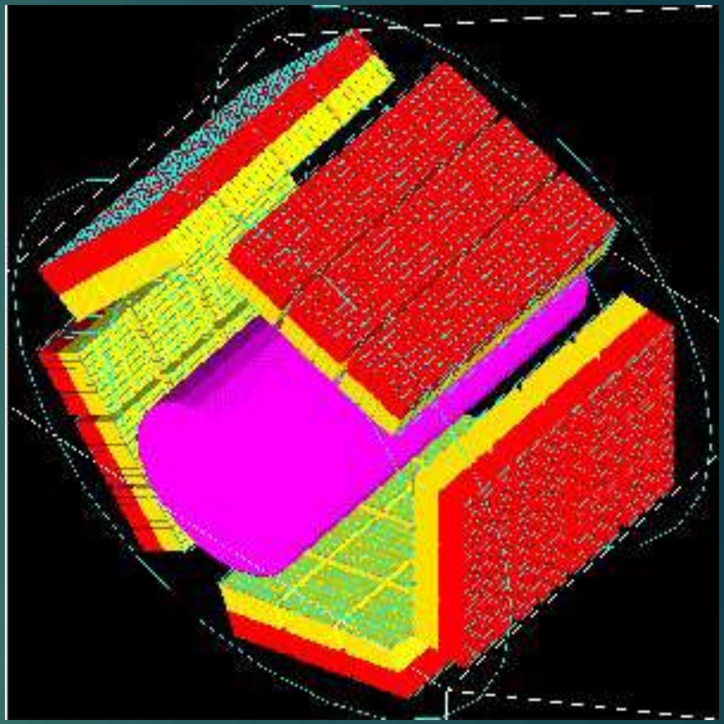

GATE generated picture of a phantom and a cylindrical PET system composed of 5 radial sectors, 4 modules (repeated along Z axis), 3 submodules (repeated along Y axis), 64 crystals (8 x 8) and 2 scintillating crystal layers (red and yellow) Source: Ref 14)

Zero-Gravity Propellant Gauging

- Methods for propellant gauging in gravity field are not effective in zero-G conditions – liquid level not identifiable
- Traditional methods of zero-G propellant gauging are subject to 3% uncertainty and greater as well as other drawbacks
  - Equation-of-state (EOS) estimations (usually the ideal gas law)
    - Pressure and temperature of the ullage volume in the tank is monitored – used to calculate volume based on EOS.
    - Requires the additional hardware of pressurant tanks, pumps, valves and other hardware necessary to transfer pressurant
  - Measurement of spacecraft dynamics
    - Propulsion system activated and spacecraft dynamics measured – used to determine over all mass of the spacecraft
    - Mass estimated by removing dry mass of spacecraft from overall mass estimation.
    - Consumes Propellant
  - Burn-time Integration.
    - Book-keeping method - Total propellant usage is estimated via assumptions about the propellant use during each thruster firing
    - Subject to large uncertainties from assumptions about thruster operating performance

Propellant Distribution in quiescent zero-G state

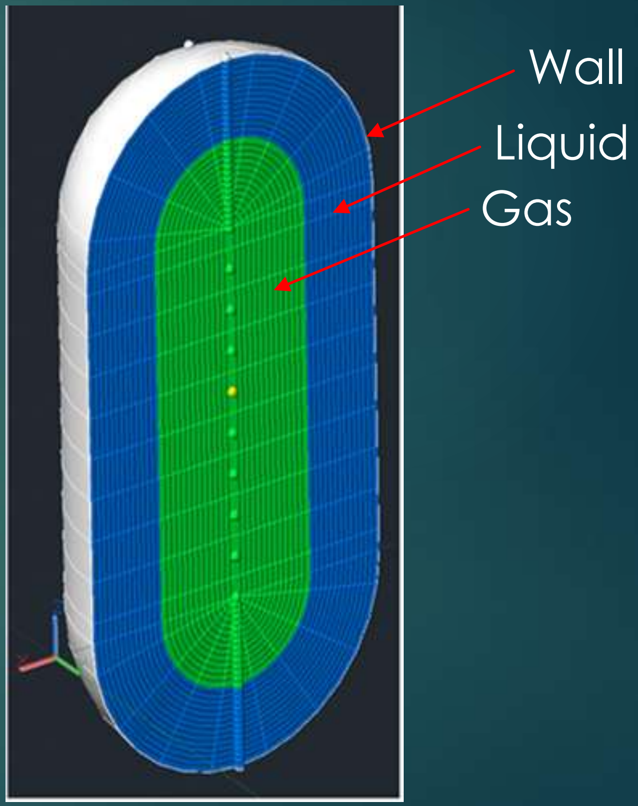

Zero-Gravity Propellant Gauging with PET

- Concept Description
  - Concept 1:
    - Saturate Fuel and/or NTO bulk propellant with Kr-79
    - Analogous to the mercaptan additive introduced to natural gas to give it an odor for easier detection.
  - Concept 2:
    - Inject Kr-79 into ullage volume
  - Utilize state of the art in PET time-of-flight (TOF) gamma ray detectors to triangulate gamma-gamma (511 keV) emission sources
  - Kr-79: 35 hr. half-life – 17 days of mission coverage
- Propellant Gauging Algorithm
  - 2D mapping of the liquid-gas interface through cross-sectional slice of tank at detector planes → Onboard algorithm generates 3D axisymmetric projection
  - Onboard void fraction algorithm used to calculate volumetric measurement of propellant.
  - Create test-validated models of void fraction vs propellant quantity.
  - Integrate sensor and model results to determine correction factors for increased accuracy.

Notional Detector Configuration

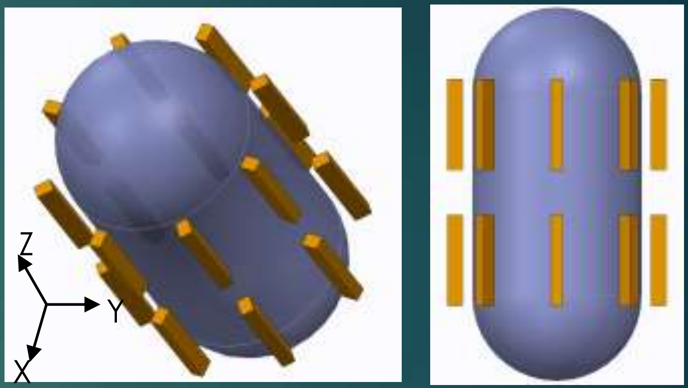

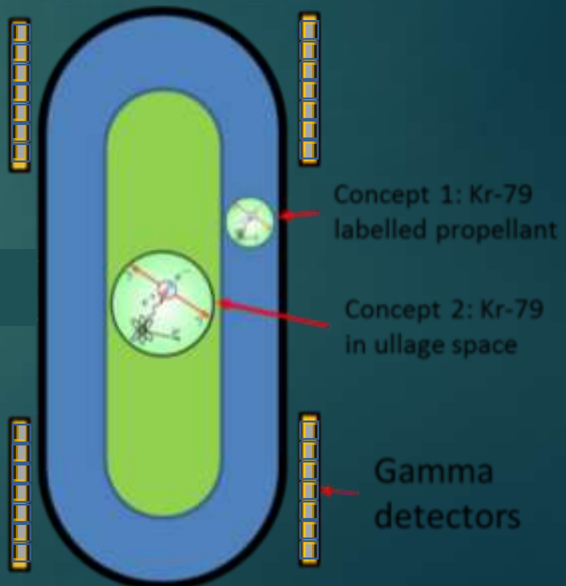

Planar Cross Section

Assessment Plan

- Objective:
  - Evaluate the ability of the shown detector configuration and proposed algorithm to accurately (< 3% uncertainty of full scale) measure the quantity of propellant in the tank.
- Approach:
  - Use GATE to simulate various detector configurations and source distributions
    - Source distributions will vary to represent multiple fill levels
      - Full, Half Full, Near Empty
    - Radioisotope concentrations, i.e. specific activity levels, will vary to represent measurement acquisitions at various points during the mission
      - Start of Mission (Day 1), Mid Mission (Day 8), End of Mission (Day 17)

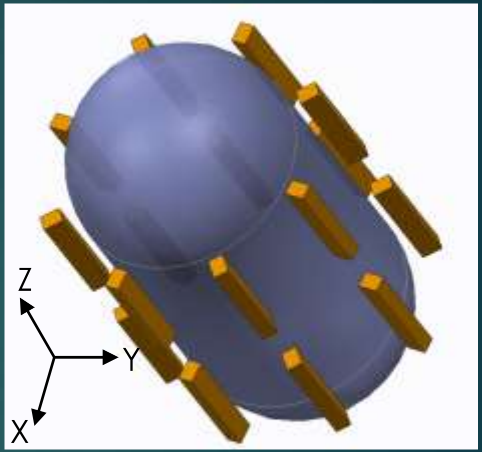

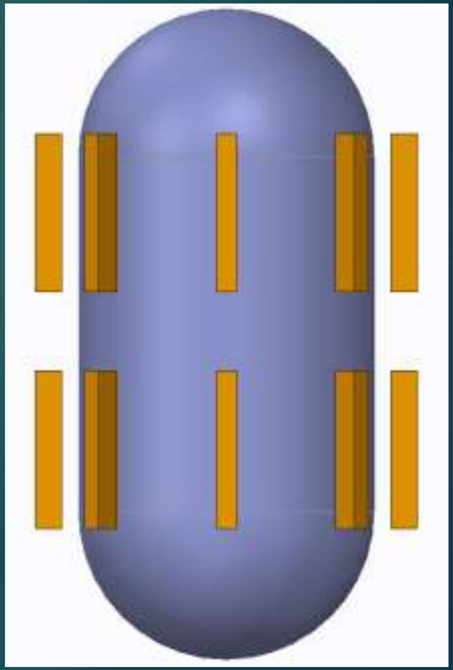

Future Work

STEADY STATE AND PERIODICALLY TRANSIENT FLOW FIELD VISUALIZATION

Electric Propulsion Devices

- Propellant:
  - Xenon, Krypton, Iodine
- Technical Challenge:
  - Results from modeling indicate that there is as much as 6% variation in maximum thrust efficiency simply due to the method of ionization.
  - Currently it is not apparent how or where this loss can be measured in thruster data.
- Possible Solution:
  - Ionization Efficiency characterization using Positron emission tomography
  - β+ Radioisotope of bulk propellant
    - Kr-79: Half Life: 35 hrs

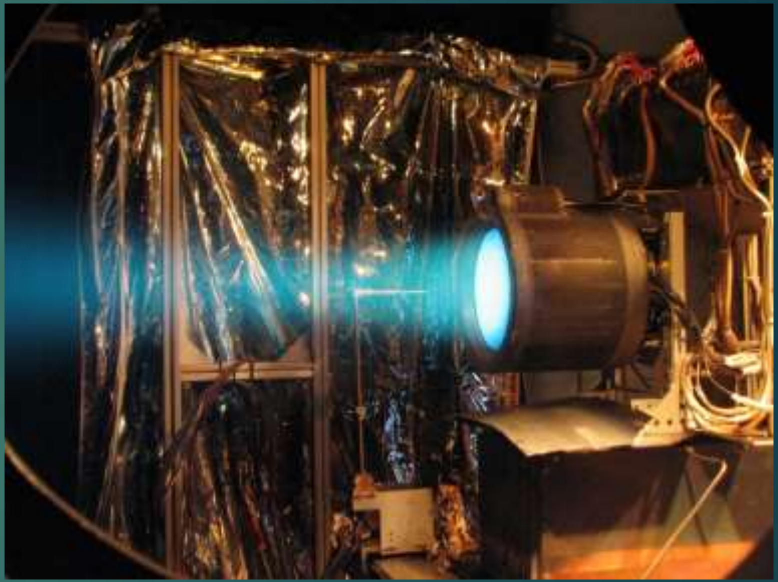

NASA JPL developed ion thruster during a test firing. A quartet of these highly efficient T6 thrusters is being installed on ESA's BepiColombo spacecraft to Mercury. (source: Ref. 15)

Concept Description

- Positron-electron annihilation occurs only once positron kinetic energy is sufficiently reduced through interactions with surrounding atoms
- Coulombic forces from propellant ions repel positrons
  - Reduces resident time near electron orbitals of ionic atoms
  - Reduces positron-electron annihilation cross-section
  - Results in correlation between localized detection rate and local ionization level

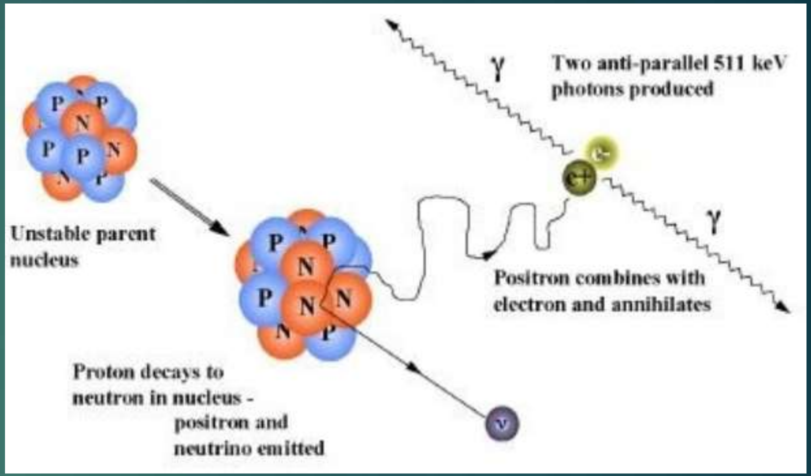

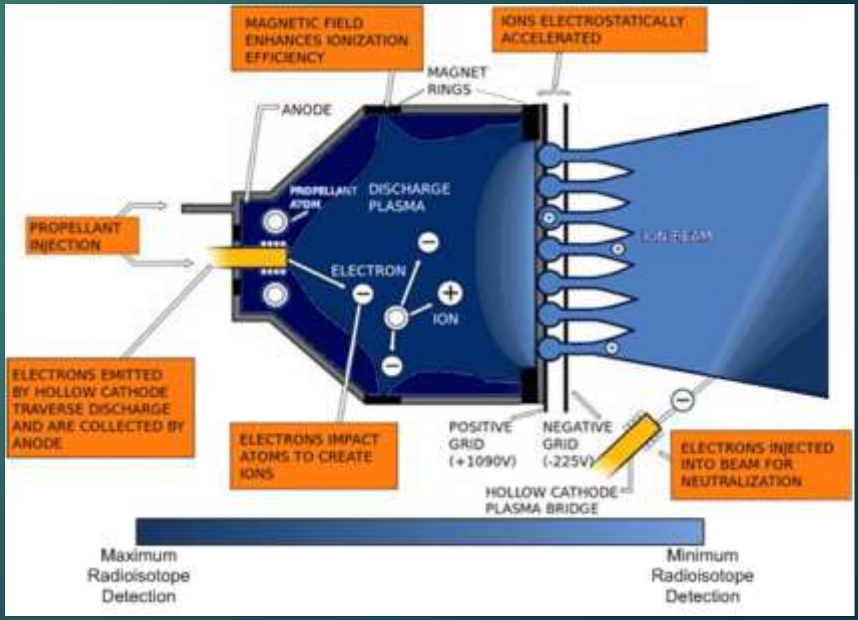

Anticipated Radioisotope detection mapping in an ion thruster using Positron Emission Tomography. (Modified from Ref. 16)

Broader Industrial Applications

- Flow feature/obstruction Characterization
  - Steady-state flow continuous radioisotope injection
- Phase Averaging of pulsed radioisotope injection
  - Flow field velocimetry using pulsed radioisotope injection
  - Periodically transient flow feature characterization

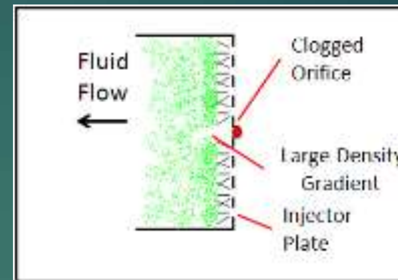

Conceptual density gradient rocket engine diagnostic application.

Flow obstruction visualization proof of concept test apparatus

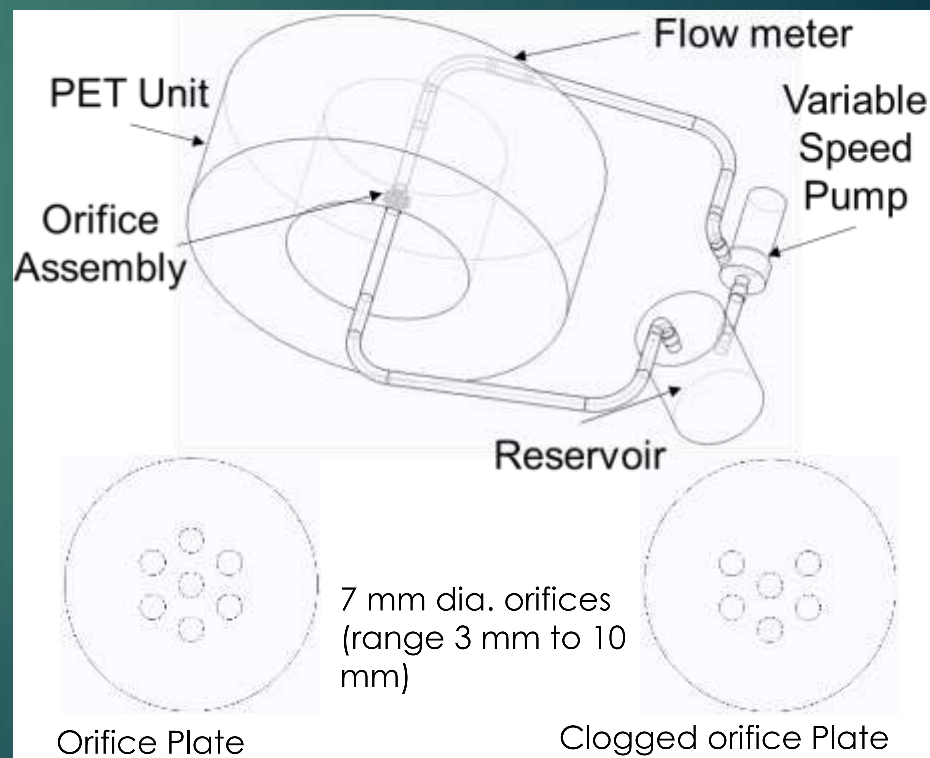

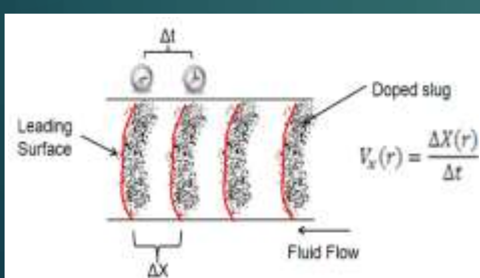

Conceptual technique for flow field velocity mapping using phase averaging of pulsed radioisotope injection

References

1. "Tracer Laser Induced Fluorescence." *Universität Duisburg-Essen*, March 17, 2014. Web. June 12, 2015
2. Dai, Jian, *et al.* "Experimental investigations of coaxial injectors in a laboratory-scale rocket combustor." Aerospace Science and Technology, Vo. 59, (Dec. 2016) Pages 41-51
3. Suleman Surti, Austin Kuhn, Matthew E. Werner, Amy E. Perkins, Jeffrey Kolthammer, and Joel S. Karp. "Performance of Philips Gemini TF PET/CT Scanner with Special Consideration for Its Time-of-Flight Imaging Capabilities." *Journal Nucl* Med, (2007); 48:471–480
4. Stewart, P. A. E. "Neutron and Positron Techniques for Fluid Transfer System Analysis and Remote Temperature and Stress Measurement." Jounal of Engineering for Gas Turbines and Power. 110.2 (1988): 279-288. Print.
5. D J Parker, TWLeadbeater, X Fan, M N Hausard, A Ingram and Z Yang. "Positron imaging techniques for process engineering: recent developments at Birmingham." Meas. Sci. Technol. 19 (2008)
6. Nuclear Physics Research Group. "Positron Imaging Centre." *University of Birmingham – Nuclear Physics Research Group*. July 6th, 2012. Web. June 14, 2015 url: http://www.np.ph.bham.ac.uk/pic/pept
7. Leadbeater T.W. and Parker D.J., "Current Trends in Positiron Emission Particle Tracking." 7th World Congress on Industrial Process Tomography, WCIPT7, 2-5 September 2013, Krakow, Poland
8. Wikipedia contributors. "Positron emission tomography." Wikipedia, The Free Encyclopedia. Wikipedia, The Free Encyclopedia, 19 May. 2015. Web. 14 Jun. 2015.

References (cont.)

9. Bailey, Dale L., et al. *Positron Emission Tomography: Basic Sciences*. London: Springer-Verlag, 2004. Print.
10. National Electronics Manufacturers Association, *NEMA NU2-2012: Performance Measurements of Positron Emission Tomography*. (2012)
11. Chang T., Chang G., Clark J.W., Jr., Diab R.H., Rohren E., Mawlawi O.R., "Reliability of predicting image signal-to-noise ratio using noise equivalent count rate in PET imaging." *Med. Phys.* 39 (10), October 2012
12. M Beiberle et al, "Ultrafast electron beam X-ray computed tomography for 2D and 3D two-phase flow imaging." IEEE. (2012) Print.
13. M. M. Tukiman, et al., "CFD Simulation of Flow Through an Orifice Plate." IOP Conf. Ser.: Materials Science & Engineering, 243 (2017) paper # 012036
14. Open Gate Collaboration contributers, website: http://www.opengatecollaboration.org/home, (2017)
15. Online graphic: https://www.esa.int/spaceinimages/Images/2016/04/T6_ion_thruster_firing (2018)
16. Wikipedia contributors. (2018, April 6). Ion thruster. In *Wikipedia, The Free Encyclopedia*. Retrieved 04:47, April 24, 2018, from https://en.wikipedia.org/w/index.php?title=Ion_thruster&oldid=835093507

Backup Slides

Dynamic Resolution Requirements

- 3 scales must be considered
  - Outer scale – larger scale bulk flow dynamics, i.e. jet diameter
    - Determined through local flow width, δ, and centerline velocity, u, providing local time scale $\tau \equiv \delta/u$
    - Results in outer scale Reynolds Number

$$Re_\delta = u\delta/\nu$$

    where ν is kinematic viscosity
  - Inner Scale – finest length scales associated variations occurring in the scalar field with respect to a Lagrangian reference frame
    - Determined by competing viscous diffusion and scalar diffusion effects
    - Spatial resolution requirement for scalar field: $\Delta x \ll \lambda_D$ (Scalar Diffusion Characteristic length)
    - Defined by: $\frac{\lambda_\nu}{\delta} = \Lambda {Re_\delta}^{-3/4}$ and $\frac{\lambda_\nu}{\lambda_D} = Sc^{-\frac{1}{2}}$

      where $Sc = \nu/D$, D is diffusivity coefficient, and Λ = 11.2 for locally defined δ
  - Advective Scale – temporal resolution constrained by instrumentation frame of reference
    - Temporal resolution requirement: $\Delta t \ll \lambda_D/u$

Example of outer scale parameters for a scalar field, i.e. fuel concentration, of a jet flow

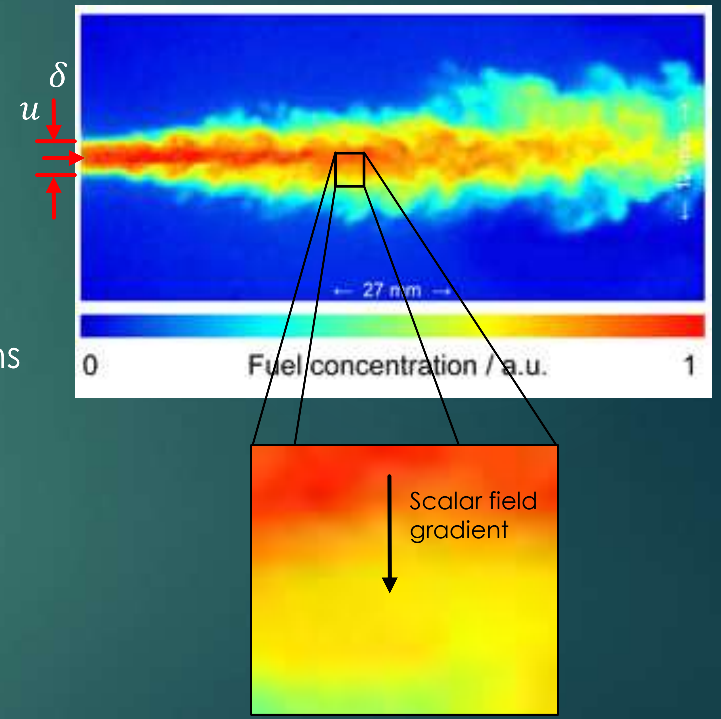

Graphic of corresponding inner scale in Lagrangian frame

Activity Concentration Optimization

- Activity Concentration Optimization
  - Preliminary effort required to determine the maximum coincidence detection rate.
  - Detector dead time, random, multiple, and scattered detections attributed to true count rates reaching a maximum value and then subsiding as activity levels increase

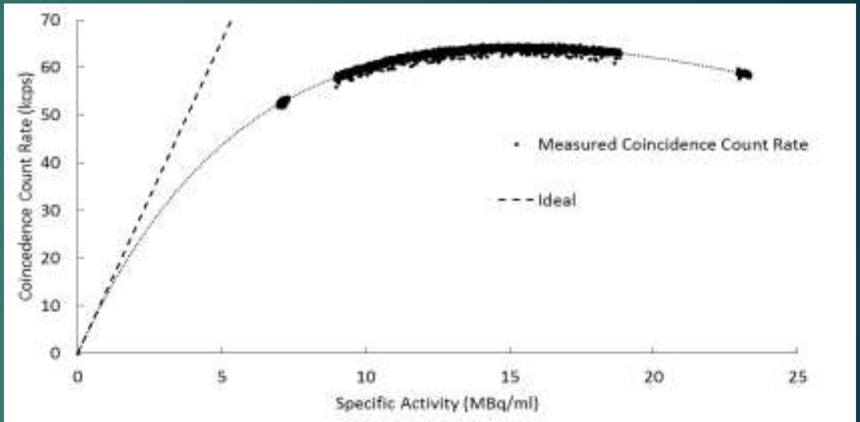

ADAC Unit optimal specific activity curve

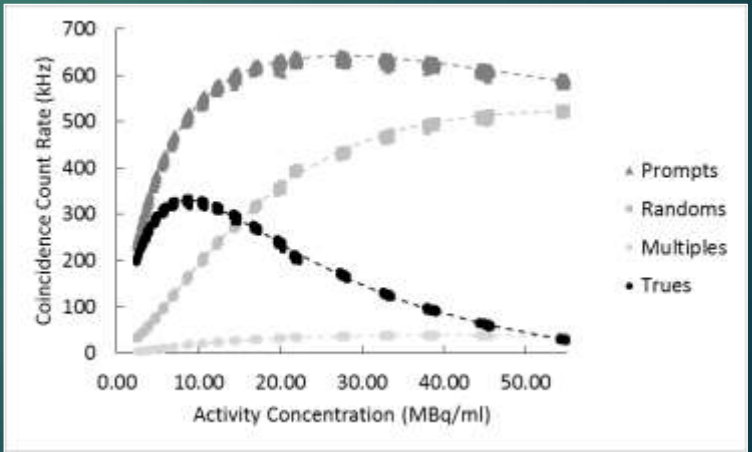

Modular Unit optimal specific activity curve